Figure S1

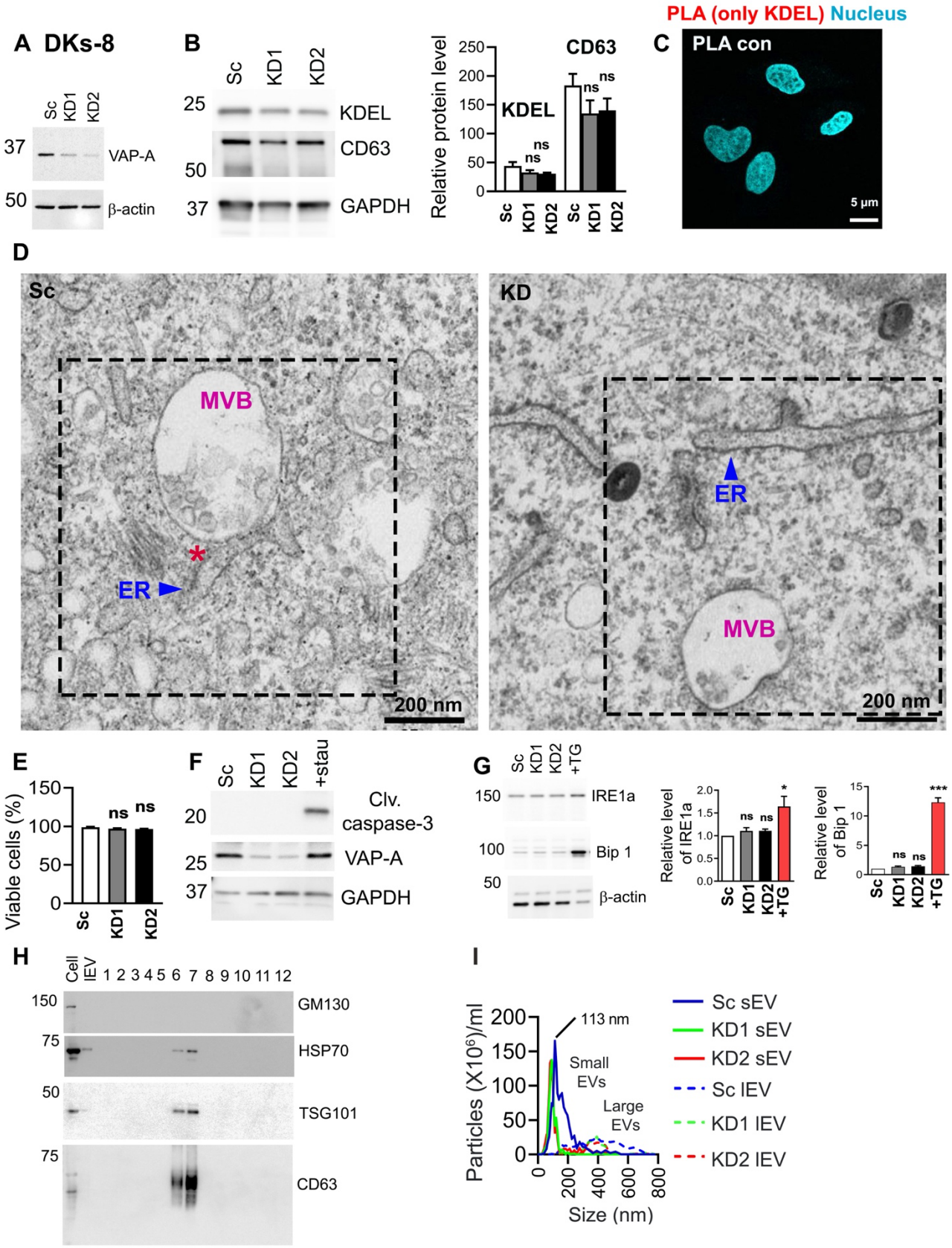
A DKs-8
Sc
KD1
KD2
37
VAP-A
50
β-actin
B
Sc
KD1
KD2
25
KDEL
CD63
50
37
GAPDH
Relative protein level
CD63
KDEL
ns
ns
ns
ns
Sc
KD1
KD2
Sc
KD1
KD2
PLA (only KDEL) Nucleus
C
PLA con
5 μm
D
Sc
MVB
ER
200 nm
KD
ER
MVB
200 nm
E
Viable cells (%)
ns
ns
Sc
KD1
KD2
F
Sc
KD1
KD2
+stau
20
Clv. caspase-3
25
VAP-A
37
GAPDH
G
Sc
KD1
KD2
+TG
150
IRE1a
100
Bip 1
50
β-actin
Relative level of IRE1a
ns
ns
*
Relative level of Bip 1
ns
ns
***
H
Cell
IEV
1 2 3 4 5 6 7 8 9 10 11 12
150
GM130
75
HSP70
50
TSG101
75
CD63
I
Particles (X10⁶)/ml
113 nm
Small EVs
Large EVs
Size (nm)
Sc sEV
KD1 sEV
KD2 sEV
Sc lEV
KD1 lEV
KD2 lEV

Figure S1. Characterization of EVs and cells upon VAP-A KD in DKs-8 cells. Related to Figure 1.

(A) Western blot analysis of VAP-A levels in control (Sc) and VAP-A KD (KD1 and KD2) DKs-8 cells. Beta actin serves as an endogenous control.

(B) Representative Western blot and quantitation of KDEL and CD63 levels for protein markers used in PLA experiments in Fig 1F. GAPDH serves as a loading control and is used to normalize levels in the graph. Quantitation from three independent experiments.

(C) Additional PLA control: KDEL only primary antibody+secondary antibodies does not yield fluorescence dots. CD63 only antibody gave similar results (not shown).

(D) Enlarged TEM images show ER and MVB membrane contact sites. Dashed boxes show the crops used for Fig 1G. Red asterisk indicates a membrane contact site in control (Sc) DKs-8 cell.

(E) Percent viability of control (Sc) and VAP-A KD (KD1, KD2) DKs-8 cells at the time of conditioned media collection. Data from three independent experiments.

(F) Representative Western blot of cleaved caspase-3, VAP-A and GAPDH in control (Sc) and VAP-A KD (KD1 and KD2) in DKs-8 cells; staurosporine (1 μM, 3h) was used as positive apoptosis inducer. Images were representative from two independent experiments.

(G) Western blot analysis of ER stress. Representative immunoblots show ER stress markers (Bip-1 and IRE1a) in control (Sc) and VAP-A KD DKs-8 cells. Thapsigargin (ER stress inducer; 10 μM, overnight) treatment of control cells serves as a positive control. Beta-actin serves as a loading control and was used to normalize the levels of IRE1a or Bip1 in the quantitation. Data from three independent experiments.

(H) Western blot analysis of positive EV markers (Hsp70, Tsg101 and CD63) and a negative EV marker (GM130) in DKs-8 cells, large EVs (lEV) and small EVs (fractions 6 and 7 of the density gradient).

(I) Graphs show nanoparticle tracking analyses (NTA) of small and large EVs isolated from control (Sc) and KD DKs-8 cells. Median of particle sizes from 3 independent experiments were combined and plotted. Note a shift in the KD small EV population towards smaller sizes.

Data plotted as Mean ± S.E.M. *$p<0.05$, **$p<0.01$, ***$p<0.001$.

Figure S2

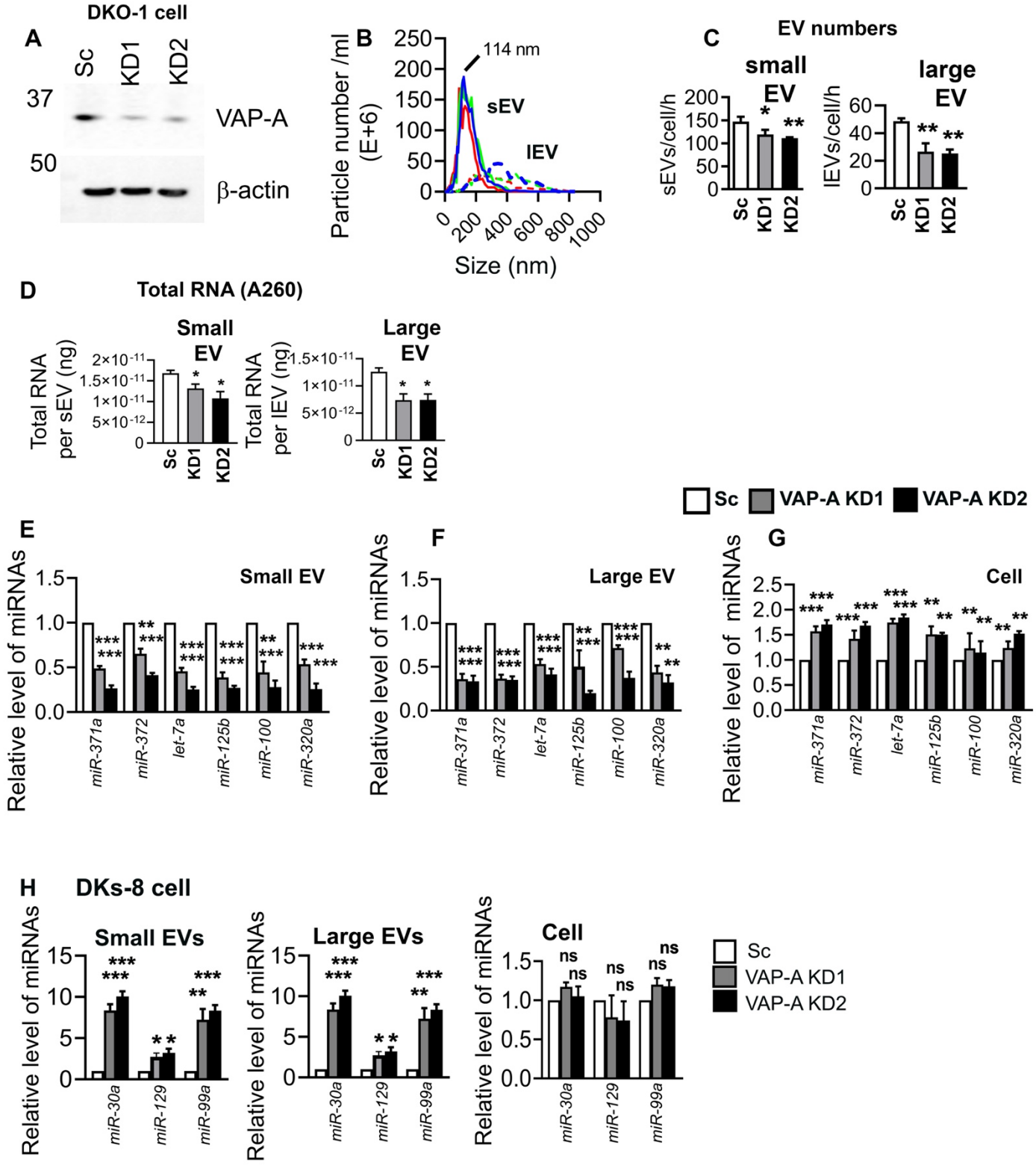
DKO-1 cell
A
Sc
KD1
KD2
37
VAP-A
50
β-actin
B
Particle number /ml (E+6)
114 nm
sEV
lEV
Size (nm)
C
EV numbers
small EV
large EV
sEVs/cell/h
lEVs/cell/h
D
Total RNA (A260)
Small EV
Large EV
Total RNA per sEV (ng)
Total RNA per lEV (ng)
Sc
VAP-A KD1
VAP-A KD2
E
Small EV
F
Large EV
G
Cell
Relative level of miRNAs
miR-371a
miR-372
let-7a
miR-125b
miR-100
miR-320a
H
DKs-8 cell
Small EVs
Large EVs
Cell
miR-30a
miR-129
miR-99a
ns

Figure S2: VAP-A controls the number and RNA content of EVs released from DKO-1 cells. Related to Figures 1 and 2.

(A) Western blot of VAP-A in DKO-1 colon cancer cells shows KD of VAP-A. Beta actin serves as a loading control.

(B) Graphs show nanoparticle tracking analyses (NTA) of small and large EVs isolated from control (Sc) and KD DKO-1 cells. Median of particle sizes from 3 independent experiments were combined and plotted.

(C) EV secretion rates calculated from NTA data for EVs isolated from control (Sc) and VAP-A KD DKO-1 cell conditioned media. Data from three independent experiments (E and F).

(D) Total RNA was extracted from a known number of purified EVs and measured by NanoDrop (A260). The concentration of RNA was plotted per small or large EV. Data from three independent experiments.

(E-G) Graphs show relative level of specific miRNAs quantified by qRT-PCR in small and large EVs purified from control (Sc) and VAP-A KD DKO-1 cells and from their respective parental cells. Data from three independent experiments.

(H) Relative levels of specific upregulated microRNAs (*miR-30a*, *miR-129*, and *miR-99*) quantified by qPCR and normalized to U6 snRNA in small and large EVs and in their parental control (Sc) or VAP-A KD DKs-8 cells. Data from three independent experiments.

Data were plotted as Mean ± S.E.M. p*<0.05, p**<0.01, p***<0.001.

Figure S3

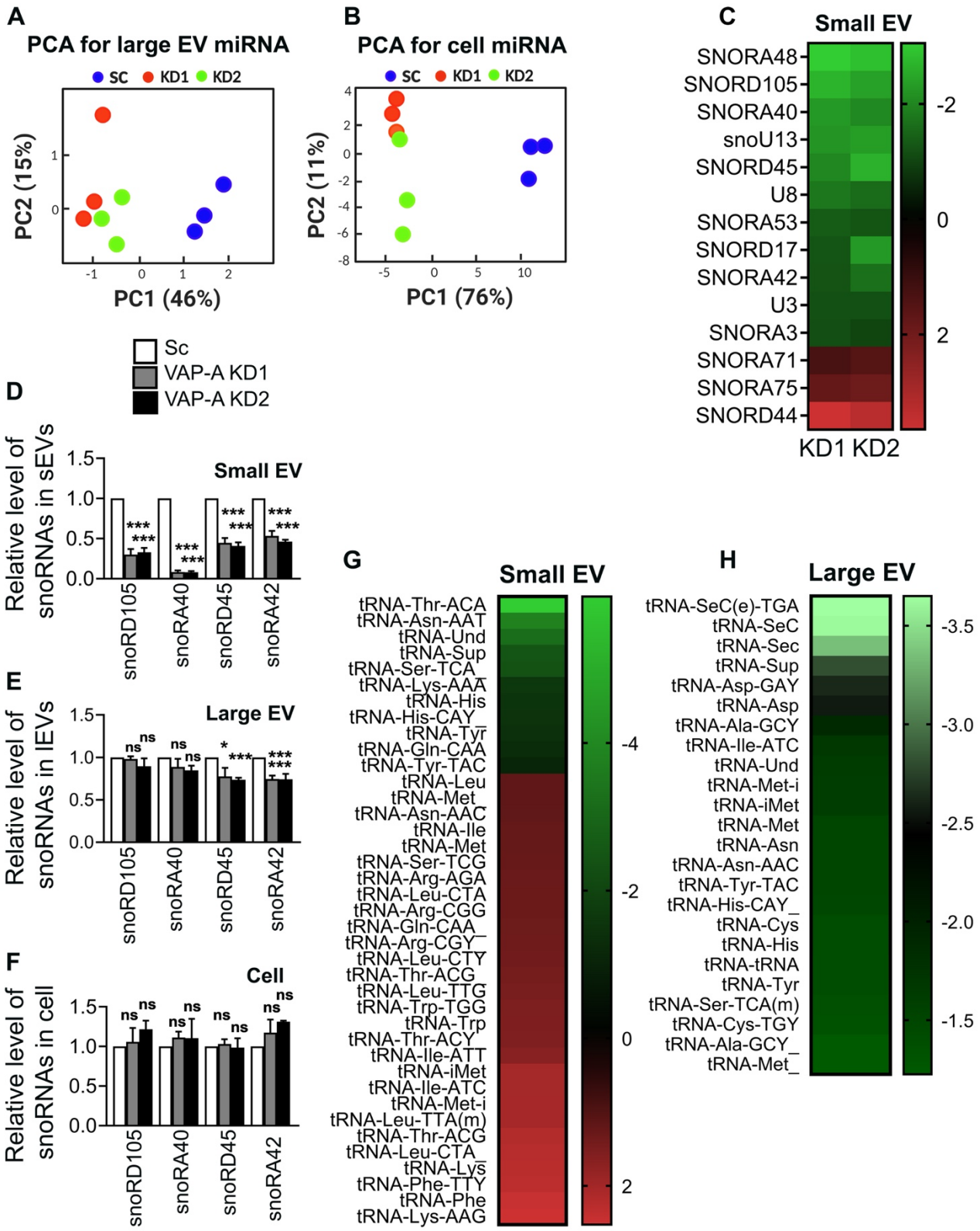
A
PCA for large EV miRNA
SC KD1 KD2
PC2 (15%)
PC1 (46%)
B
PCA for cell miRNA
SC KD1 KD2
PC2 (11%)
PC1 (76%)
C
Small EV
SNORA48
SNORD105
SNORA40
snoU13
SNORD45
U8
SNORA53
SNORD17
SNORA42
U3
SNORA3
SNORA71
SNORA75
SNORD44
KD1 KD2
Sc
VAP-A KD1
VAP-A KD2
D
Small EV
Relative level of snoRNAs in sEVs
snoRD105
snoRA40
snoRD45
snoRA42
E
Large EV
Relative level of snoRNAs in lEVs
F
Cell
Relative level of snoRNAs in cell
G
Small EV
tRNA-Thr-ACA
tRNA-Asn-AAT
tRNA-Und
tRNA-Sup
tRNA-Ser-TCA
tRNA-Lys-AAA
tRNA-His
tRNA-His-CAY
tRNA-Tyr
tRNA-Gln-CAA
tRNA-Tyr-TAC
tRNA-Leu
tRNA-Met
tRNA-Asn-AAC
tRNA-Ile
tRNA-Met
tRNA-Ser-TCG
tRNA-Arg-AGA
tRNA-Leu-CTA
tRNA-Arg-CGG
tRNA-Gln-CAA
tRNA-Arg-CGY
tRNA-Leu-CTY
tRNA-Thr-ACG
tRNA-Leu-TTG
tRNA-Trp-TGG
tRNA-Trp
tRNA-Thr-ACY
tRNA-Ile-ATT
tRNA-iMet
tRNA-Ile-ATC
tRNA-Met-i
tRNA-Leu-TTA(m)
tRNA-Thr-ACG
tRNA-Leu-CTA
tRNA-Lys
tRNA-Phe-TTY
tRNA-Phe
tRNA-Lys-AAG
H
Large EV
tRNA-SeC(e)-TGA
tRNA-SeC
tRNA-Sec
tRNA-Sup
tRNA-Asp-GAY
tRNA-Asp
tRNA-Ala-GCY
tRNA-Ile-ATC
tRNA-Und
tRNA-Met-i
tRNA-iMet
tRNA-Met
tRNA-Asn
tRNA-Asn-AAC
tRNA-Tyr-TAC
tRNA-His-CAY
tRNA-Cys
tRNA-His
tRNA-tRNA
tRNA-Tyr
tRNA-Ser-TCA(m)
tRNA-Cys-TGY
tRNA-Ala-GCY
tRNA-Met

Figure S3. VAP-A regulates the levels of small RNAs in EVs. Related to Figure 2.

(A and B) Principal component analysis (PCA) shows that VAP-A KD affects the miRNA composition of large EVs and cells.

(C) Analysis of small RNA-Seq data. Levels (log 2-fold change) of snoRNAs in small and large EVs were normalized to levels in their parental cells and then compared between control and VAP-A KD. Heatmap shows altered snoRNAs in VAP-A KD small EVs purified from DKs-8 cells using criteria ≤ 0.5 or ≥ 2 fold change and FDR value<0.05. Green shows downregulated whereas red shows upregulated RNAs. Levels plotted as log 2-fold change.

(D-F) Relative levels of specific snoRNAs quantified by qPCR and normalized to U6 snRNA in small EVs, large EVs and their parental control (Sc) or VAP-A KD DKs-8 cells, as indicated above. Data from three independent experiments.

(G and H) Heatmap analyses of small RNA-Seq data show altered tRNA fragments in small and large EVs in VAP-A KD conditions, using criteria ≤ 0.5 or ≥ 2 fold change and FDR value<0.05. Levels plotted as log 2-fold change.

Bar graphs show Mean ± S.E.M. *p<0.05, **p<0.01, ***p<0.001.

Figure S4

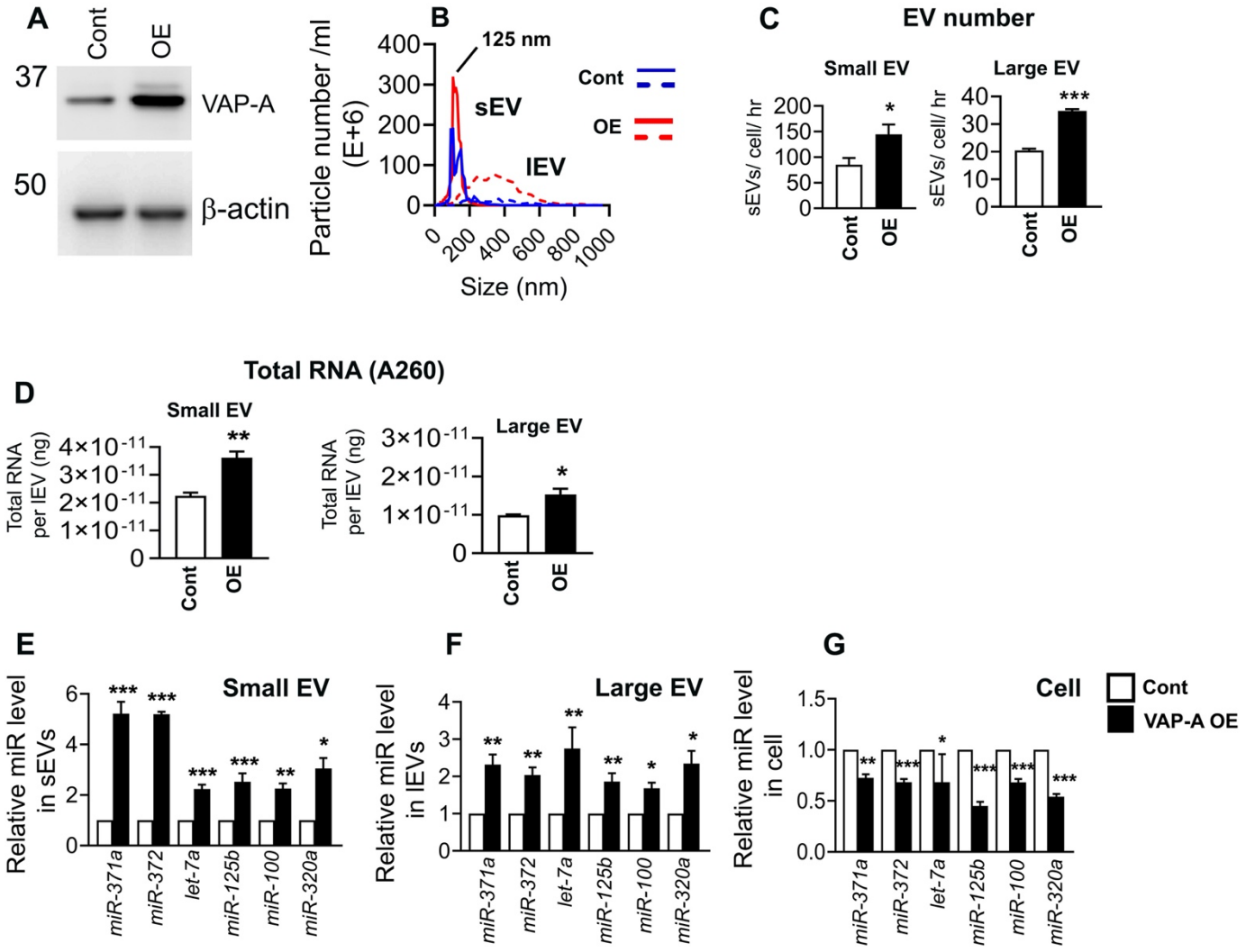

Figure S4. VAP-A overexpression enhances the number and RNA content of EVs. Related to Figures 1 and 2.

(A) Western blot of VAP-A in DKs-8 cells shows overexpression (OE) of VAP-A. Beta actin serves as an endogenous control.

(B) NTA traces from large (lEV) and small (sEV) EVs purified from control (Cont) and VAP-A OE cells. Median values were combined for each condition and plotted from three independent NTA experiments.

(C) Calculation of small and large EV secretion rate from control and VAP-OE cells based on NTA analysis of purified EVs and known cell number and media conditioning time. From three independent NTA experiments.

(D) Total RNA concentration (measured by NanoDrop (A260)) per EV (measured by NTA) for EVs purified from control and VAP-A OE DKs-8 cells.

(E-G) Relative levels of specific miRNAs in small and large EVs purified from control (Cont) and VAP-A OE (OE) DKs-8 cells and their parental cells. Data from three independent experiments.

Data were plotted as Mean ± S.E.M. *p<0.05, **p<0.01, ***p<0.001.

Figure S5

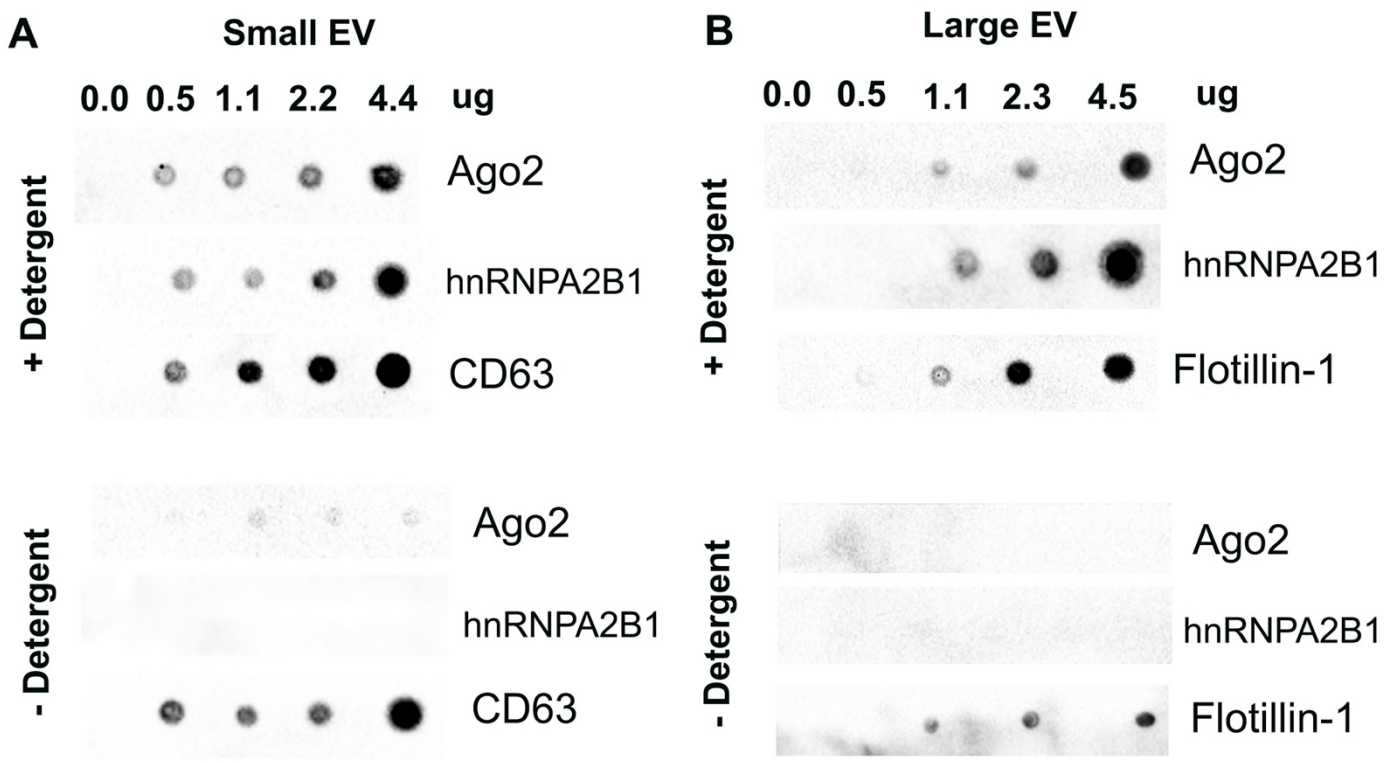

Figure S5: RBPs are present on the inside of small and large EVs. Related to Figure 2.

(A and B) Different concentrations of small and large EVs from DKs-8 cells were dotted on nitrocellulose membranes and probed with anti-Ago2, anti-hnRNPA2B1, anti-CD63 or anti-flotillin-1 antibodies in the presence (+Detergent) or absence (-Detergent) of 0.1% Tween-20 as shown. Representative of three independent experiments.

Figure S6

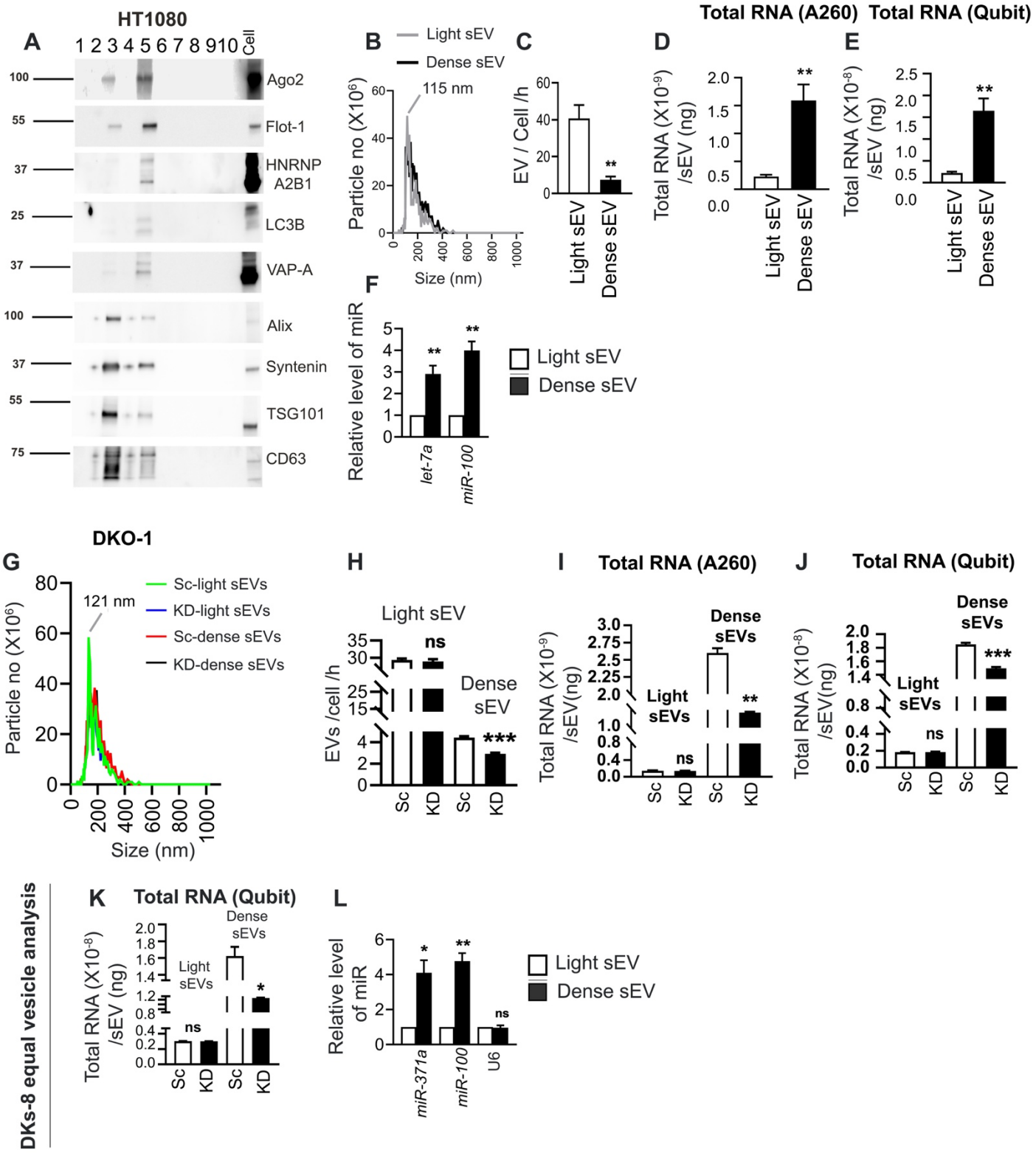
HT1080
A
1 2 3 4 5 6 7 8 9 10 Cell
100
Ago2
55
Flot-1
37
HNRNP A2B1
25
LC3B
37
VAP-A
100
Alix
37
Syntenin
55
TSG101
75
CD63
B
Light sEV
Dense sEV
115 nm
Particle no (X10^6)
Size (nm)
C
EV / Cell /h
Light sEV
Dense sEV
Total RNA (A260)
Total RNA (Qubit)
D
Total RNA (X10^-9) /sEV (ng)
E
Total RNA (X10^-8) /sEV (ng)
F
Relative level of miR
let-7a
miR-100
DKO-1
G
Sc-light sEVs
KD-light sEVs
Sc-dense sEVs
KD-dense sEVs
121 nm
H
Light sEV
Dense sEV
EVs /cell /h
ns
I
Total RNA (A260)
Light sEVs
Dense sEVs
J
Total RNA (Qubit)
DKs-8 equal vesicle analysis
K
Total RNA (Qubit)
L
Relative level of miR
miR-371a
miR-100
U6

Figure S6: Analysis and characterization of "light" and "dense" EVs. Related to Figure 3.

(A) Representative immunoblots of different EV cargo and marker proteins (Ago2, Flotillin-1, hnRNPa2b1, LC3B, VAP-A, Alix, syntenin, Tsg101 and CD63) show enrichment of different cargoes in fractions 3 and 5 of "light" and "dense" EVs purified from parental HT1080 cells. Blots representative of three independent experiments.

(B) Nanoparticle traces of "light" and "dense" small EVs purified from parental HT1080 cells.

(C) EV concentration of "light" and "dense" EVs purified from HT1080 were plotted.

(D and E) Total RNA quantity per "light" and "dense" small EV measured by A260 with NanoDrop (D) or Qubit (E) from HT1080 cells. Data from three independent experiments.

(F) Relative levels of *let-7a* and *miR-100* were calculated for light and dense small EVs purified from HT1080 and plotted. U6 serves as endogenous control that remains unchanged. Data were calculated from three independent experiments with three technical replicates.

(G) Nanoparticle traces of "light" and "dense" small EVs purified from parental DKO-1 cells.

(H) EV concentration of "light" and "dense" EVs purified from DKO-1 cells were plotted.

(I and J) Total RNA quantity per "light" and "dense" small EV measured by A260 with NanoDrop (I) or Qubit (J) from DKO-1 cells. Data from three independent experiments.

(K) Total RNA was extracted from equal number of "light" and "dense" vesicles purified from DKs-8 cells and measured by Qubit and plotted as RNA per vesicle. Data from three independent experiments.

(L) Graph shows relative level of *miR-371*, *miR-100* and U6. QRT-PCR were performed with equal volume of total RNA extracted from equal "light" and "dense" EVs purified from DKs-8 cells. Data were calculated from three independent experiments with three technical replicates.

Data were plotted as Mean ± S.E.M. *$p<0.05$, **$p<0.01$, ***$p<0.001$.

Figure S7

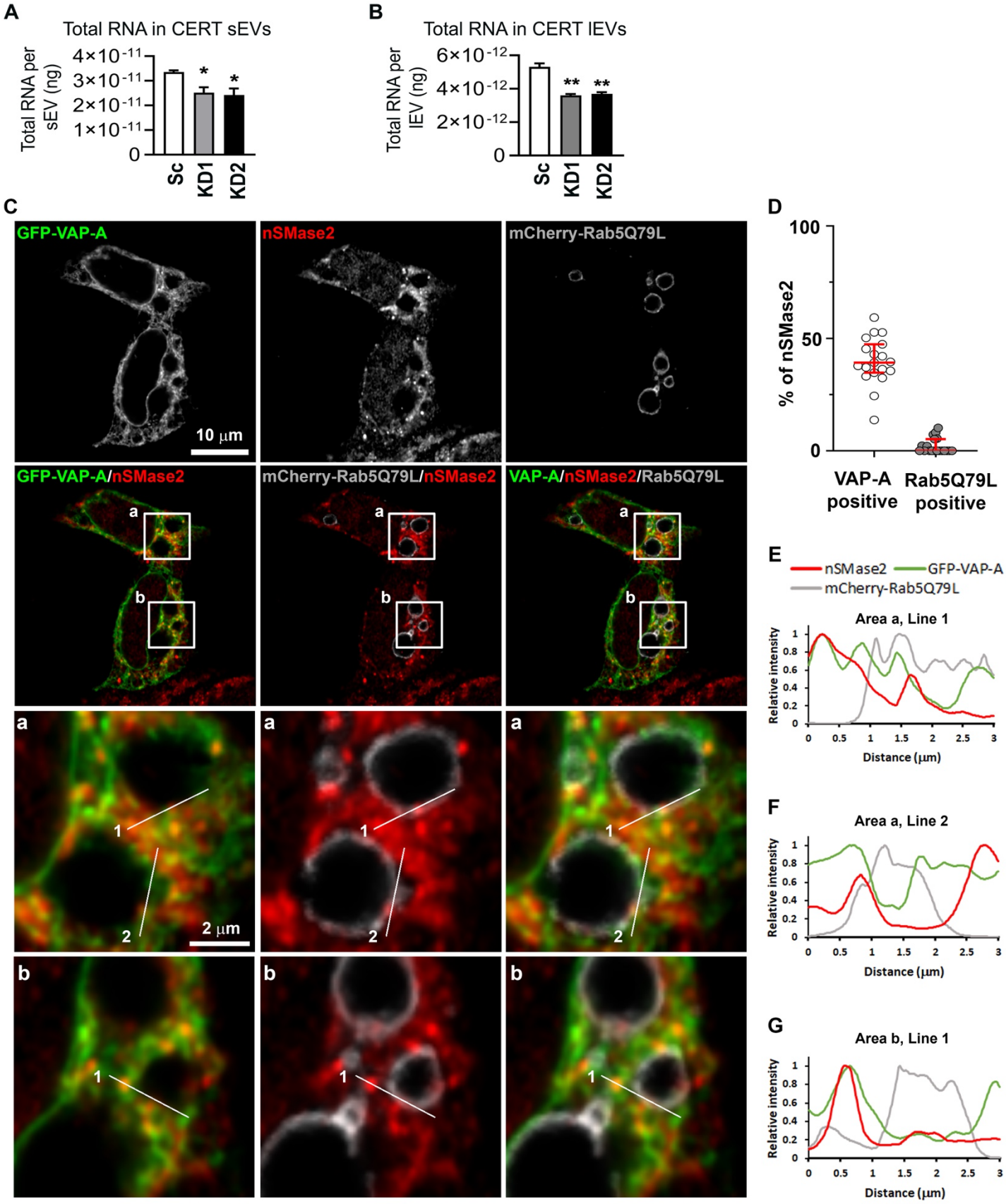
A
Total RNA in CERT sEVs
Total RNA per sEV (ng)
4×10-11
3×10-11
2×10-11
1×10-11
0
*
*
Sc
KD1
KD2
B
Total RNA in CERT IEVs
Total RNA per IEV (ng)
6×10-12
4×10-12
2×10-12
0
**
**
Sc
KD1
KD2
C
GFP-VAP-A
nSMase2
mCherry-Rab5Q79L
10 μm
GFP-VAP-A/nSMase2
mCherry-Rab5Q79L/nSMase2
VAP-A/nSMase2/Rab5Q79L
a
b
1
2
2 μm
D
% of nSMase2
100
50
0
VAP-A positive
Rab5Q79L positive
E
nSMase2
GFP-VAP-A
mCherry-Rab5Q79L
Area a, Line 1
Relative intensity
Distance (μm)
F
Area a, Line 2
Relative intensity
Distance (μm)
G
Area b, Line 1
Relative intensity
Distance (μm)

Figure S7. nSMase2 is closely associated with VAP-A-positive ER. Related to Figure 7.

(A and B) Total RNA quantity per small and large EV purified from control (Sc) and CERT KD (KD1 and KD2) were calculated and plotted from three independent experiments as mean ± S.E.M. *p<0.05, **p<0.01

(C) Representative merged (not deconvolved) image of GFP-VAP-A and mCherry-Rab5Q79L-cotransfected DKs-8 cells with nSMase2 immunofluorescence staining. Lettered and selected areas are enlarged at the bottom. Numbered lines were scanned for the intensity of each fluorescence channel of the images and plotted at (E-G).

(D) Colocalization of nSMase2 with GFP-VAP-A and mCherry-Rab5Q79L was plotted as median with interquartile range, respectively. *n* = 19 cells from 2 independent experiments.